

# Effects of Pouring Temperature on Interfacial Reaction between Ti-47.5Al-2.5V-1Cr Alloy and Mold during Centrifugal Casting

SUI Yanwei, FENG Kun, CHENG Cheng, CHEN Xiao, QI Jiqui\*, HE Yezeng, MENG Qingkun, WEI Fuxiang, SUN Zhi

(School of Materials Science and Engineering, China University of Mining and Technology, Xuzhou 221116, China)

**Abstract:** Pouring temperature and time are the most important influencing factors on interfacial reaction during the centrifugal casting. When cast at high temperatures, the crucible becomes brittle and prone to cracking, and shows a low stability. In this paper, we studied the centrifugal casting of Ti-47.5-Al-2.5V-1Cr alloy, and explored the effects of pouring temperature on the interfacial reaction. Castings at 1 600, 1 650, and 1 700 °C were obtained by controlling the other parameters constant in the experiments. The microstructure, elemental distribution, thickness of the reaction layer and phase composition of the castings at the interface were studied. The results show that the thickness at the interfacial reaction layer is increased by raising the pouring temperature. The elements in the mold and the matrix were double-diffused and reacted at the interface during the casting process, and formed solid solutions with the precipitation of many new phases such as Al<sub>2</sub>O<sub>3</sub> and TiO<sub>2</sub>. The roughness of interface structure and layer thickness of reaction increase with the rise of temperature, and the interfacial reaction is more intense. There is a minimum layer thickness of the reaction layer that is 80 μm when the temperature is 1 600 °C.

**Key words:** TiAl alloy; centrifugal casting; interfacial reaction; pouring temperature

## 1 Introduction

With the development of the aerospace, automotive and other industries, the need for high-performance materials is also increasing<sup>[1,2]</sup>. TiAl alloy gains growing importance as raw materials in these industries because of a low density and higher mechanical property at ambient and elevated temperatures<sup>[3,4]</sup>. The  $\gamma$ -TiAl alloy exhibits satisfactory stable performance by its mature production technology<sup>[5]</sup>.

Centrifugal casting is widely used in the  $\gamma$ -TiAl alloy casting process<sup>[6,7]</sup> owing to the reduction of shrinkage, inclusions as well as other defects and the improvement of the matrix organization<sup>[8,9]</sup>. Recent studies particularly focus on the too thick casting layer,

slow performance and other issues of  $\gamma$ -TiAl alloy reacting with mold<sup>[10]</sup>. Therefore, it is significant to explore the other influence factors in the interfacial reaction layer during the casting process.

Pouring temperature is an important process parameter as it plays a key role on the formation of cast microstructure and the thickness of the interfacial reaction layer during the centrifugal casting<sup>[11,12]</sup>. More recent studies about influence of the other process parameters in the casting process are shown below. Ni-44Ti-5Al-2Nb-1Mo alloy has been melted at different temperatures with a constant pulling rate in directional solidification<sup>[13]</sup>. Alloys with Ti-45Al-8.5Nb composition during directional solidification have been cast by changing the pulling rate at a temperature gradient of 3.8 K/mm<sup>[14]</sup>. However, the effects of pouring temperature on the interfacial reaction between TiAl alloy and the mold in centrifugal casting have been rarely studied. There is no systematic research on the effect of temperature on interfacial reactions. Therefore, no guidance on production is available. In this paper, we studied the effects of pouring temperature on the interfacial reaction between the Ti-45Al-8.5 Nb alloy and the mold during centrifugal casting.

©Wuhan University of Technology and SpringerVerlag Berlin Heidelberg 2016

(Received: Oct. 20, 2015; Accepted: June 4, 2016)

SUI Yanwei (隋艳伟): Assoc. Prof.; Ph D; E-mail: 15852187006@163.com

\*Corresponding author: QI Jiqui (戚继球): Assoc. Prof.; Ph. D; E-mail: fkqianxian@126.com

Funded by the National Natural Science Foundation of China(No. 51304198) and Natural Science Foundation of Jiangsu Province (Nos. 2013106, 20141134 and 2014028-08)

## 2 Experimental

### 2.1 Raw materials

The chemical composition of smelting TiAl alloy in this study is tabulated in Table 1. The alloy ingots were smelted in an argon tungsten-arc smelting furnace and then recast. The castings (1#, 2#, 3#) were obtained respectively at different pouring temperatures (1 600, 1 650, 1 700 °C) during centrifugal casting, while keeping the centrifugal speed at 600 r/min and the centrifugal radius at 55 mm. When the temperature decreased below 50 °C, the ingots were removed from the furnace and cleaned carefully. Then the casts were cut with wire cutting technology in the corresponding position on the casts, and the size of each sample is 10 mm×10 mm× 10 mm. Then after 5 min of washing with acetone, the samples were removed from the ultrasonic cleaning machine.

**Table 1 Chemical composition of smelting TiAl alloy**

Ti	Al	V	Cr	others
48%	47.5%	2.5%	1%	≤1%

**Table 2 Ingredients of the mold surface slurry**

Compo- sition	ZrO <sub>2</sub>	Y <sub>2</sub> O <sub>3</sub>	Latex	TiO <sub>2</sub>	Yttrium sol	Deionized water	Wetting agent
Percent- age/%	7.3	70.7	2	4	7.9	5.1	0.2

The mold material was zirconia, and the binders of the surface and back layers were fabricated by yttrium and silica sol respectively. The above materials were calcined in an electric furnace at 950 °C, and then the molds were formed after 2 h of incubation. The ingredients of the mold surface slurry are shown in Table 2, and the preparation process is elaborated as follows. After the mixer was stabilized, a desired amount of deionized water was weighed and poured into a paint bucket at the rotational speed of 3 000 r/min and stirred. Then fused yttria and zirconia powders (9:1) were added to form a suspension, followed by the addition of TiO<sub>2</sub> powder, latex, yttrium sol and other materials. The pH of the configuring slurry should be between 9 and 10, so it can be dewaxed after drying.

### 2.2 Analysis procedures

The hardness at the interface between the base alloy and the mold was detected by a Vickers micro-hardness tester with a 5 kg load for 10 s. The measurement was first conducted at 5 μm away from the sample surface, and then a test point was set at each 25 μm along a line until the point 180 μm away from the sample surface. The phases were examined using a D8 Advance diffractometer with Cu Kα radiation at 40

kV and 30 mA in X-ray diffraction (XRD) experiments. In addition, microstructure and elements distribution at the interface were detected using a scanning electron microscope (SEM, FEI QuantaTM250) and an energy dispersive spectrometer (EDS, Quantax 400-10) respectively.

## 3 Results

### 3.1 Effects of pouring temperature on microhardness

The hardness distribution on the casting interface at different pouring temperatures is shown in Fig.1. The thickness of the reaction layer can be estimated by the distance between the casting surface and the area where the hardness tends to smooth down<sup>[15]</sup>. Clearly, the hardness of all samples is reduced with increasing distance from the casting interface, and finally the values stabilize. As showed in Fig. 1, the thickness of the reaction layer increases with the rise of casting temperature. The thickness of the reaction layer was maximized to about 140 μm at pouring temperature 1 700 °C and minimized to about 70 μm at 1 600 °C.

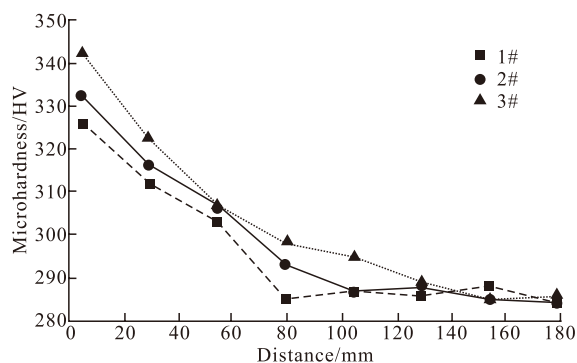


Fig.1 Hardness distribution of casting interface at different pouring temperature

### 3.2 Morphology and elemental distribution at the interface

The reaction layer and the base portion as well as their boundary can be clearly seen from the SEM photographs (Fig.2). A part of the reaction layer fell off during the preparation process, which proves its brittleness. The diffusion distances of Y, Zr and other elements are short, while those of Ti, Al, and V are relatively longer. Simultaneously, Ti, Al, O and other elements fluctuated due to the existence of pits at the reaction layer on surface. These fluctuations occur during the line scanning experiments, mostly because the data collection in those places is insufficient.

The elements Ti and Al are rarely present in the reaction layer with the low diffusion extent of O, and a completely smooth interface with a less appropriate extent of interface reaction appears (right side of

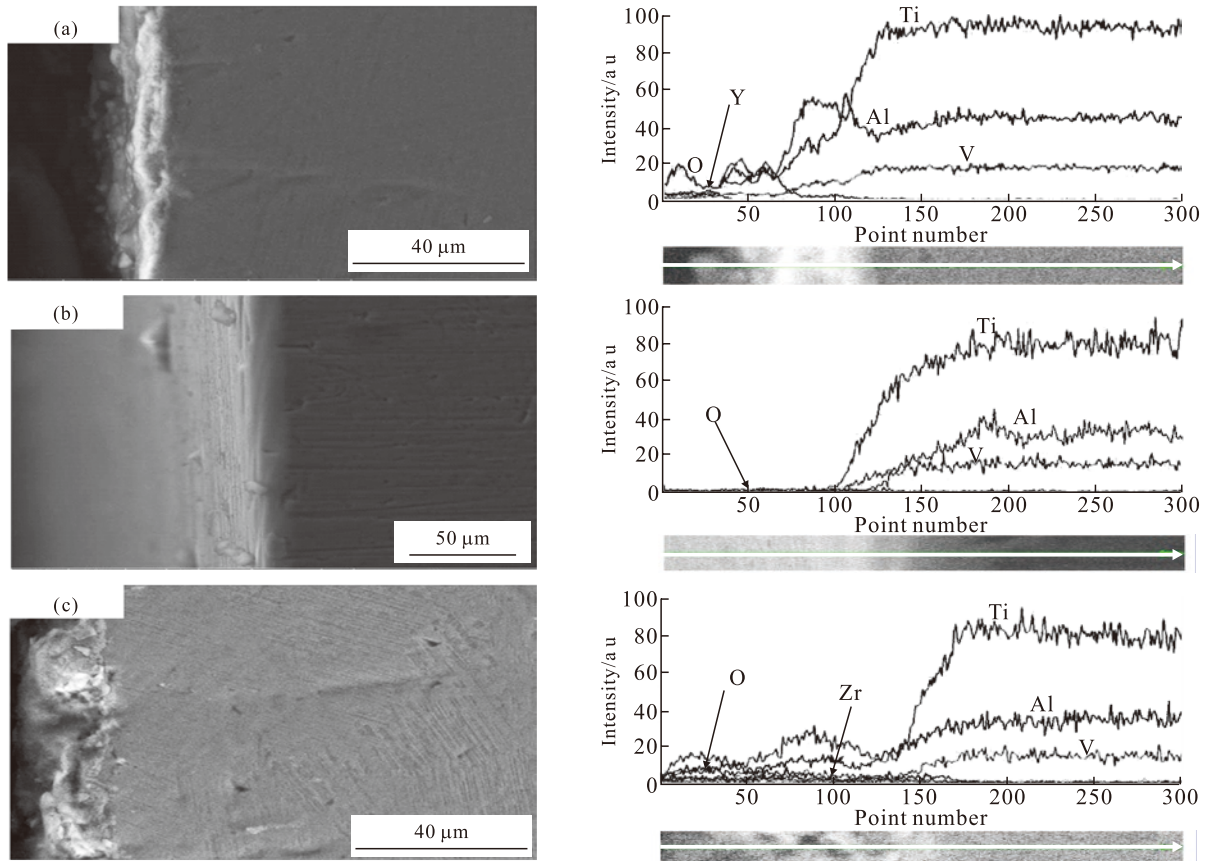


Fig.2 SEM and EDS results under the condition of different samples: (a) 1#; (b) 2#; (c) 3#c

Fig.2(b)). Y, O, Ti, Al and other elements dissolved and diffused reciprocally, resulting in a violent reaction at the interface (right side in Figs.2(a) and 2(c)). The reaction generated many hard phases and solid solutions with higher intensity<sup>[16]</sup>. Combined with Fig.2, the distance between the casting surface and the place with Ti and Al content changes can be seen as the thickness of the reaction layer. The estimations of distances show that the rising pouring temperature can exacerbate the interfacial reaction and increase the thickness of the reaction layer, which is consistent with the microhardness test.

### 3.3 Phase identification at the interface

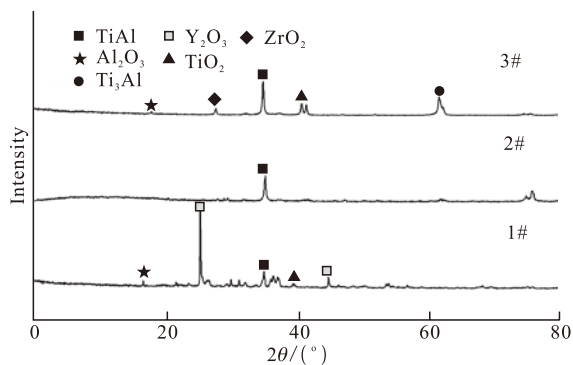


Fig.3 XRD patterns of different samples at the interface

Fig.3 presents the XRD patterns of different samples at the interface. Clearly,  $ZrO_2$ ,  $Y_2O_3$ ,  $TiO_2$ ,

$Ti_3Al$  and  $Al_2O_3$  were generated without the presence of Zr or Y. Specifically, Y and Zr completely penetrated into the matrix through the interface reaction with the substrate, and then the interfacial reaction layer formed. In this process, no element existed at the reaction layer where many new phases and solid solutions were generated.

More complex interfacial reaction occurred at the interface with increasing pouring temperature. Only  $TiO_2$ ,  $Y_2O_3$ ,  $Al_2O_3$  and other oxides were generated at low pouring temperature, and  $Ti_3Al$ ,  $ZrO_2$  and other new phases were precipitated at the pouring temperature of 1700 °C. The left side of Fig.2(c) shows a rougher microstructure with serious peeled particles and more intense reaction at the interface<sup>[15]</sup>.

## 4 Discussion

$ZrO_2$  and  $Y_2O_3$  decomposed at high temperatures in molding material as shown in Formulas (1) and (2):



With  $Y_2O_3$  for example, the equilibrium constant is shown in Eq.(3):

$$K = \alpha^2(Y)\alpha^3(O)/\alpha(Y_2O_3) \quad (3)$$

where  $K$  is only related to the temperature at the interface<sup>[17]</sup>.  $K$  would be correspondingly larger at a higher temperature at the interface, and more  $Y_2O_3$  will be exploded into the TiAl alloy matrix. Conversely, the decreased temperature at the interface led to the reduced decomposition amount of  $Y_2O_3$ , and  $Y_2O_3$  dissolved in the melt would precipitate at the interface. The increasing pouring temperature prolonged the residence time of the alloy in the liquid region, and provided the grains also with enough time for nucleation and growth. A uniform lamellar structure was generated during the solidification (the left side in Fig.2). Even small strips and diffused tissues were observed. By the melt erosion, the elements Y, Zr and O diffused into the substrate and reacted at the interface with Ti, Al and other elements in the substrate, in which many new phases were generated (Fig.3).

During the centrifugal casting, the reduction of pouring temperature is equivalent to increasing the cooling rate<sup>[18]</sup>. The transfer of heat and mass in this process was reduced with the decrease of pouring temperature. O is highly soluble in TiAl alloys, and its atomic radius is relatively small, which leads to a stronger diffusion capacity than that of Y and Zr in the reaction layer. However, the TiAl alloy contains a large amount of Al, and Al can strongly inhibit the melting activity. As a result, Al can modestly inhibit the reaction and diffusion of O with the matrix, while Ti, Al and other elements in the matrix can also diffuse into the mold. Al only needs to overcome a small diffusion barrier owing to the small atomic radius, which leads to the faster diffusion rate. New phases were generated at the interface due to the mutual diffusion and reaction of the elements, which shows a higher hardness than matrix. In comparison, the inter-diffusion of elements at the interface caused a part of free atoms to form solid solutions on the casting surface, and the hardness is also slightly larger than that in the matrix<sup>[19]</sup>. Therefore, the hardness generally declines along the interface to the inner substrate (Fig.1).

## 5 Conclusions

During the centrifugal casting, the elements in the mold and the matrix were double-diffused and reacted at the interface, which led to the generation of the interfacial reaction layer.

The thickness of the interfacial reaction layer was improved with the increase of the pouring temperature. The thickness of the reaction layer was minimized to about 70  $\mu\text{m}$  at 1 600 °C. Meanwhile, a variety of new solid solutions and phases such as  $TiO_2$ ,  $Al_2O_3$ , and

$Ti_3Al$  were generated at the interface.

## References

- [1] Zhang H R, Gao M, Tang X X, et al. Interaction between Ti-47Al-2Cr-2Nb Alloy and  $Y_2O_3$  Ceramic During Directional Solidification [J]. *Acta Metall. Sin.*, 2010, 46(7): 890-896
- [2] Cui Y, Tang X, Gao M, et al. Interactions between TiAl Alloy and Different Oxide Moulds under High-temperature and Long-time Condition[J]. *High Temperature Materials and Processes*, 2013, 32(3): 295-302
- [3] Zhao E, Kong F, Chen Y, et al. Interfacial Reactions between Ti-1100 Alloy and Ceramic Mould During Investment Casting[J]. *Transactions of Nonferrous Metals Society of China*, 2011, 21: 348-352
- [4] Luo W Z, Shen J, Min Z X, et al. Investigation of Interfacial Reactions between TiAl Alloy and Crucible Materials During Directional Solidification Process[J]. *Rare Metal Materials and Engineering*, 2009, 8: 031
- [5] Jia L, Xu D, Li M, et al. Casting Defects of Ti-6Al-4V Alloy in Vertical Centrifugal Casting Processes with Graphite Molds[J]. *Metals and Materials International*, 2012, 18(1): 55-61
- [6] Ma X, Mei Z. Structure and Mechanical Properties of Al-based Gradient Composites Reinforced with Primary Si and  $Mg_2Si$  Particles through Centrifugal Casting[J]. *Journal of Wuhan University of Technology-Mater. Sci. Ed.*, 2013, 28(4): 813-818
- [7] Bo L I, Kai W, Liu M, et al. Effects of Temperature on Fracture Behavior of Al-based *in-situ* Composites Reinforced with  $Mg_2Si$  and Si Particles Fabricated by Centrifugal Casting[J]. *Transactions of Nonferrous Metals Society of China*, 2013, 23(4): 923-930
- [8] Huang X, Liu C, Lu X, et al. Aluminum Alloy Pistons Reinforced with SiC Fabricated by Centrifugal Casting[J]. *Journal of Materials Processing Technology*, 2011, 211(9): 1 540-1 546
- [9] Sui Y W, Li B S, Liu A H, et al. Physical Simulation of Infiltration Flow during Centrifugal Casting Titanium Alloy Melts Feeding[J]. *Rare Metal Materials and Engineering*, 2009, 38(9): 1 537-1 541
- [10] Pan Q, Zheng L, Sang Y, et al. Effect of Casting Temperature on Microstructure in a Directionally Solidified Ni-44Ti-5Al-2Nb-1Mo Alloy[J]. *Rare Metals*, 2011, 30(1): 349-353
- [11] Samadi A, Shahbazzkhani H R. Effect of Pouring Temperature and Casting Thickness on Distribution Gradient of *in Situ* Formed  $Al_2Cu$  Particles During Centrifugal Casting of Hypereutectic Al-Cu Alloy[J]. *International Journal of Cast Metals Research*, 2014, 27(3): 129-134
- [12] Sui Y W, Yuan F, Li B S, et al. Physical Simulation Similar Theory and Experiment during Centrifugal Casting Ti Alloy Melts Filling Flow[J]. *Rare Metal Materials and Engineering*, 2012, 41(8): 1 351-1 356
- [13] Ding X F, Lin J P, He J, et al. Directional Solidification of Ti-45Al-8Nb- (W,B,Y) Alloy[J]. *Rare Metals*, 2010, 29(3): 292-297
- [14] Ding X F, Lin J P, Qi H, et al. Microstructure Evolution of Directionally Solidified Ti-45A-8.5 Nb-(W,B,Y) Alloys[J]. *Journal of Alloys and Compounds*, 2011, 509(9): 4 041-4 046
- [15] Wang Z J, Du J L, Li Z L, et al. Influence of Sintering Temperature on the Structure and High-temperature Discharge Performance of  $LiNi_{1/3}Mn_{1/3}Co_{1/3}O_2$  Cathode Materials[J]. *Journal of Wuhan University of Technology-Mater. Sci. Ed.*, 2015, 30(5): 894-899
- [16] Ding H S, Nie G, Chen R R, et al. Influence of Oxygen on Microstructure and Mechanical Properties of Directionally Solidified Ti-47Al-2Cr-2Nb Alloy[J]. *Materials & Design*, 2012, 41: 108-113
- [17] Yang H M, Su Y Q, Luo L S, et al. Influences of Fe and B on the Columnar Structure of Ti-46Al Alloys[J]. *Rare Metal Materials and Engineering*, 2012, 41(4): 570-574
- [18] Liu Z, Mao W M, Liu X M. Effect of Pouring Temperature on Fractal Dimension of Primary Phase Morphology in Semi-solid A356 Alloy[J]. *Transactions of Nonferrous Metals Society of China*, 2009, 19(5): 1 098-1 103
- [19] Zhang F Y, Cheng H, Xu Y K, et al. Influence of Mo Content on Microstructure and Microhardness of Laser Solid Formed Ti-6Al-Mo System Alloys[J]. *Rare Metal Materials and Engineering*, 2013, 42(7): 1 332-1 336